Multifunctional Composites: Optimizing Microstructures for Simultaneous Transport of Heat and Electricity

S. Torquato,[1,2] S. Hyun,[1] and A. Donev[1,3]

[1]*Princeton Materials Institute, Princeton University, Princeton, New Jersey 08544*

[2]*Department of Chemistry, Princeton University, Princeton, New Jersey 08544*

[3]*Program in Applied & Computational Mathematics, Princeton University, Princeton, New Jersey 08544*

(Received 10 June 2002; published 9 December 2002)

Composite materials are ideally suited to achieve multifunctionality since the best features of different materials can be combined to form a new material that has a broad spectrum of desired properties. Nature's ultimate multifunctional composites are biological materials. There are presently no simple examples that rigorously demonstrate the effect of competing property demands on composite microstructures. To illustrate the fascinating types of microstructures that can arise in multifunctional optimization, we maximize the simultaneous transport of heat and electricity in three-dimensional, two-phase composites using rigorous optimization techniques. Interestingly, we discover that the optimal three-dimensional structures are bicontinuous triply periodic minimal surfaces.

DOI: 10.1103/PhysRevLett.89.266601 PACS numbers: 72.80.Tm, 62.20.Dc

Increasingly, a variety of performance demands are being placed on material systems. These include materials with desirable mechanical, thermal, electromagnetic, optical, chemical, and flow properties, and low weight [1,2]. It is difficult to find homogeneous materials that possess these multifunctional characteristics. Composite materials (mixtures of two or more different materials) are ideally suited to achieve multifunctionality since the best features of different materials can be combined to form a new material that has a broad spectrum of desired properties. The ultimate multifunctional materials are provided by nature; virtually all biological material systems are composites that typically are endowed with a superior set of properties. This is undoubtedly due to the fact that biological systems must be able to perform a variety of functions well; i.e., roughly speaking, biological materials are ''optimized'' for multifunctional purposes. Currently, there are no simple examples that rigorously demonstrate the effect of competing property demands on composite microstructures. In this Letter, we provide the first such examples using optimization techniques.

To illustrate the fascinating types of microstructures that can arise in multifunctional optimization, we consider the simultaneous transport of heat and electricity in three-dimensional, two-phase composites [3]. Both phases exist in equal proportions such that phase one is a good thermal conductor but poor electrical conductor and phase two is a poor thermal conductor but good electrical conductor. Demanding that the sum of the effective thermal and electrical conductivities is maximized sets up a *competition* between the two effective properties. (If we maximized only one of the conductivities, say, thermal conductivity, then the well-known Hashin-Shtrikman singly coated sphere structures [4] in which the conducting phase two is connected and the less conducting phase one is disconnected is an optimal solution.)

Here we adapt the topology optimization method [5–7] for this multifunctional optimization. To date, the topology optimization technique has been used to extremize a *single* effective property. We have discovered that certain single-scale bicontinuous structures maximize the sum of the two effective conductivities and the effective properties obtained lie on a rigorous cross-property upper bound. A *bicontinuous* composite is one in which both phases are connected across the sample. Interestingly, the optimal bicontinuous structures turn out to be triply periodic *minimal* surfaces.

A minimal surface is a surface that is locally area minimizing. Minimal surfaces necessarily have zero mean curvature; i.e., the sum of the principal curvatures at each point is zero. Particularly fascinating are minimal surfaces that are triply periodic. These structures are bicontinuous in the sense that the surface divides space into two disjointed regions that are simultaneously continuous. Triply periodic minimal surfaces arise in a variety of applications, including self-assembly processes in block copolymers [8], nanocomposites [9], micellar materials [10], and lipid-water systems [11].

In general, it is desired to design a composite material with N different effective properties or responses, which we denote by $K_e^{(1)}, K_e^{(2)}, \ldots, K_e^{(N)}$, and to know the region (set) in the multidimensional space of effective properties in which all composites must lie (see Fig. 1). The size and shape of this region depends on the specification of the phase properties and level of microstructural information. The determination of the allowable region is generally a highly complex problem. However, the identification of the allowable region can be greatly facilitated if *cross-property* bounds on the effective properties can be found. Cross-property bounds are inequalities that rigorously link different effective properties to one another (e.g., links between different transport

properties [12–15] and between the conductivity and elastic moduli [16]). When cross-property bounds are optimal, they can be used to identify the boundary of the allowable region. Numerical optimization methods can then be used to find specific microstructures that lie on the boundary.

Here we specifically consider a two-phase composite material in which phase i has electrical conductivity σ_i, thermal conductivity λ_i, and volume fraction ϕ_i, where $i = 1$ or 2. Cross-property bounds exist between the effective electrical conductivity σ_e and thermal conductivity λ_e. Bergman [12] derived the following cross-property bound:

$$\frac{\lambda_2 - \lambda_1}{\lambda_e - \phi_1\lambda_1 - \phi_2\lambda_2} - \frac{\sigma_2 - \sigma_1}{\sigma_e - \phi_1\sigma_1 - \phi_2\sigma_2} = \frac{3(\lambda_2\sigma_1 - \lambda_1\sigma_2)}{\phi_1\phi_2(\lambda_2 - \lambda_1)(\sigma_2 - \sigma_1)}. \tag{1}$$

Relation (1) gives an upper (lower) bound when the sign of $(\lambda_2\sigma_1 - \lambda_1\sigma_2)/(\sigma_1 - \sigma_2)$ is positive (negative). Milton [13] conjectured and Avellaneda *et al.* [14] proved that Bergman's corresponding lower bound (not presented) for isotropic media can be improved [when $(\lambda_2\sigma_1 - \lambda_1\sigma_2)/(\sigma_1 - \sigma_2)$ is positive] by the realizable and thus optimal bound

$$\frac{\sigma_1 + 2\sigma_2}{\sigma_1 - \sigma_2}\left(\frac{\sigma_2 + 2\sigma_1}{\sigma_1 - \sigma_2} - \phi_2\frac{\sigma_e + 2\sigma_1}{\sigma_1 - \sigma_e}\right) = \frac{\lambda_1 + 2\lambda_2}{\lambda_1 - \lambda_2}\left(\frac{\lambda_2 + 2\lambda_1}{\lambda_1 - \lambda_2} - \phi_2\frac{\lambda_e + 2\lambda_1}{\lambda_1 - \lambda_e}\right). \tag{2}$$

The reciprocal bound (1) was shown by Milton to be optimal at five distinct points on this bound. One of these points corresponds to a special *bicontinuous multiscale* composite: a polycrystal in which each grain is composed of a laminate consisting of alternating slabs of phases one and two such that the slab thicknesses are much smaller than the size of the grain and the grains are randomly oriented [17]. The effective conductivity of such a statistically isotropic polycrystal has an effective electrical conductivity $\sigma_e = \sigma_*(\phi_2)$, where

$$\sigma_*(\phi_2) = \phi_1\sigma_1 + \phi_2\sigma_2 - \frac{\phi_1\phi_2(\sigma_2 - \sigma_1)^2}{3(\phi_1\sigma_2 + \phi_2\sigma_1)}. \tag{3}$$

We emphasize that this point lies on Bergman's bound.

Figure 2 shows the lens-shaped region defined by the cross-property bounds (1) and (2) in the σ_e-λ_e plane at a volume fraction $\phi_2 = 1/2$ for a case of "ill-ordered" phases ($\sigma_1/\sigma_2 < 1$ and $\lambda_1/\lambda_2 > 1$) in which

$$\sigma_1 = 0.1, \qquad \sigma_2 = 1.0, \qquad \lambda_1 = 1.0, \qquad \lambda_2 = 0.1. \tag{4}$$

The datum (filled circle) on the upper bound corresponds to the aforementioned *bicontinuous* composite. The question is whether there is a bicontinuous *single-length scale* structure that achieves the same point on the upper bound.

To answer this question, we carried out a multifunctional optimization by maximizing the objective function

$$\Phi = \lambda_e + \sigma_e \tag{5}$$

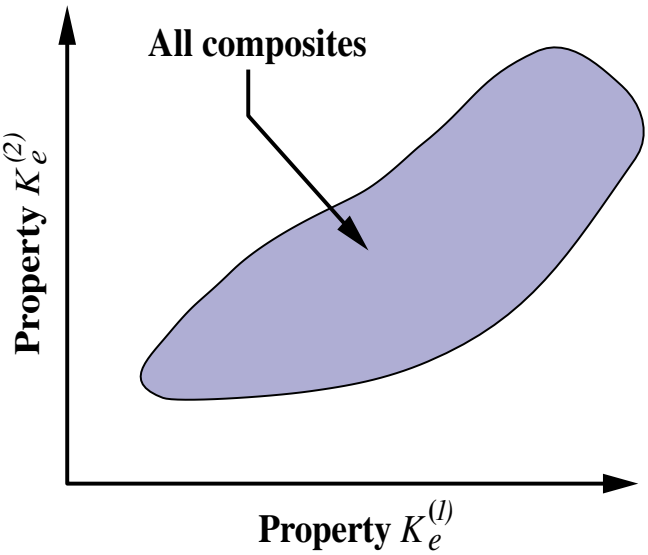

FIG. 1 (color online). Schematic illustrating the allowable region in which all composites, with specified phase properties and microstructural constraints, must lie for the case of two different effective properties.

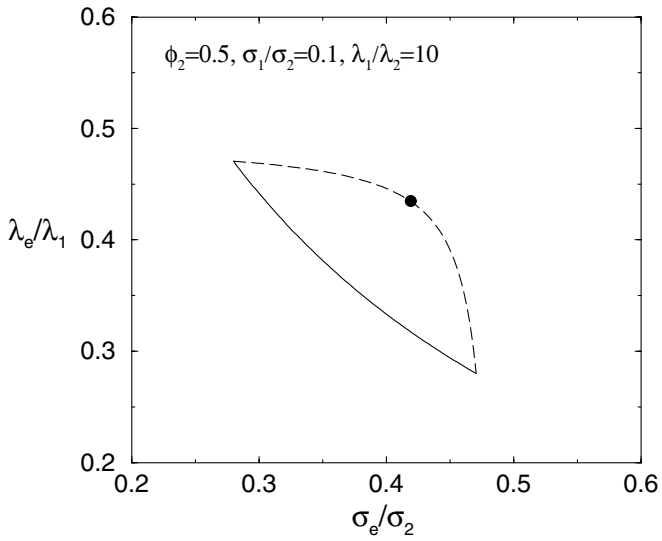

FIG. 2. Cross-property bounds and simulation datum for the effective electrical σ_e and thermal λ_e conductivities for ill-ordered phases ($\sigma_1/\sigma_2 < 1$ and $\lambda_1/\lambda_2 > 1$) as specified by (4). The datum on the upper bound corresponds to the bicontinuous structures described in the text. Elsewhere [18] we have shown that the two points corresponding to the intersections of the upper and lower bounds are three-dimensional generalizations of the two-dimensional single-scale Vigdergauz structures [19].

for a volume fraction $\phi_1 = \phi_2 = 1/2$ and ill-ordered phases as specified by (4). Thus, phase one has a high thermal conductivity but low electrical conductivity and phase two has a low thermal conductivity but high electrical conductivity. The optimization problem is solved numerically by adapting the topology optimization technique [6,7]. Briefly, the design domain is digitized into a large number of finite elements, and periodic boundary conditions are used. The effective property at any step is obtained by averaging (homogenizing) the relevant fields. The microstructure evolves using well-established linear programming techniques until the objective function is extremized (see Refs. [6,7] for further details). The unit domain was chosen to be a cube and was digitized into small cubic finite elements ($40 \times 40 \times 40$). Geometric symmetry (threefold reflection) was imposed to ensure isotropy of the effective conductivity tensors.

We find that an optimal composite is a bicontinuous structure, as shown in Fig. 3. Bicontinuity allows the structure to maximize both properties for the case of *ill-ordered* phases. This topological feature (i.e., percolation of both phases) is virtually unique to three dimensions [2]. Note that this bicontinuous structure achieves the datum (within small numerical error) shown in Fig. 2 for the cross-property upper bound on the sum of the two conductivities in which $\lambda_e/\lambda_2 = \sigma_e/\sigma_1 = 0.427$. Although we take $\phi_1 = \phi_2 = 1/2$, the topological property of bicontinuity will extend to other volume fractions.

Based on visual inspection of the optimal structure produced via the topology optimization method, we hypothesize that the bicontinuous structure is a Schwartz primitive (P) surface, a well-known triply periodic minimal surface with simple cubic symmetry. To verify that this, indeed, is a Schwartz P minimal surface, we must find an exact representation of it and then compute its effective properties. Minimal surfaces can be characterized exactly using a Weierstrass (complex integration) representation, but in practice this is difficult to use numerically. Instead, we utilize a Landau free-energy type model [20] to calculate numerically a discretization of a potential $\psi(x)$ such that $\psi(x) > 0$ for points in phase one and $\psi(x) < 0$ for points in phase 2. At the phase interface, $\psi(x) = 0$, which in this case is a Schwartz P minimal surface.

We obtained the data for this potential (from the authors of Ref. [19]) on a 64^3 unit cell as well as one for another minimal surface with macroscopically isotropic effective conductivities, namely, the Schwartz diamond (D) surface (see Fig. 4). From these potentials, one can readily make discretizations of bicontinuous two-phase composites having a minimal surface as the two-phase interface boundary. We then used a finite-element code to calculate numerically the effective conductivities of these composites. Remarkably, we found that the computed conductivities for *both Schwartz P and D surfaces* matched the ones predicted by the cross-property upper bound up to three decimal places for case (4). Importantly, we also computed the effective conductivities for a wide range of phase contrasts, including the infinite-contrast case ($\sigma_1/\sigma_2 \to 0$, $\lambda_1/\lambda_2 \to \infty$) and found the same agreement with the corresponding analytical results. This provides strong evidence that these minimal surfaces indeed realize the upper bound (within numerical error), independent of the phase contrast.

One may ask how minimal surfaces arise when "surface tension" is absent in our problem. In order to begin to answer this question one should note that the case examined here represents a special point on the cross-property upper bound (see Fig. 2). The phase volume fractions are identical ($\phi_1 = \phi_2$), and the dimensionless conductivities are identical ($\sigma_e/\sigma_2 = \lambda_e/\lambda_1$). Thus, the system possesses *phase-inversion symmetry;* i.e., the morphology of phase one is identical to the morphology of phase two [21]. We also know that if optimal single-scale structures exist, they must be bicontinuous composites. Moreover, in our numerical optimization study, we imposed simple cubic symmetry. In summary, an optimal composite should be bicontinuous, possess phase-inversion symmetry at a volume fraction $\phi_1 = \phi_2 = 1/2$, and possess simple cubic symmetry. The Schwartz P surface

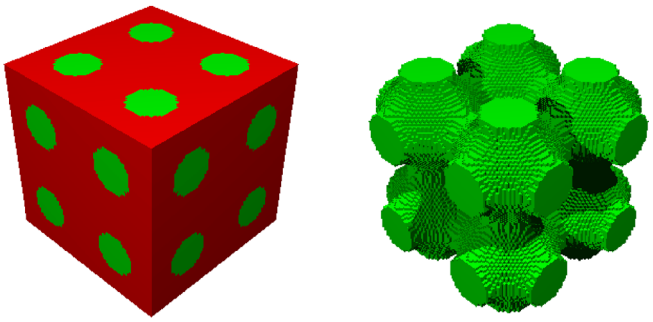

FIG. 3 (color online). A bicontinuous optimal structure at $\phi_1 = \phi_2 = 1/2$ corresponding to maximization of the sum of the effective electrical and thermal conductivities ($\sigma_e + \lambda_e$) for ill-ordered phases as specified by (4). Left panel: A $2 \times 2 \times 2$ unit cell of the composite. Right panel: Corresponding morphology of phase 2.

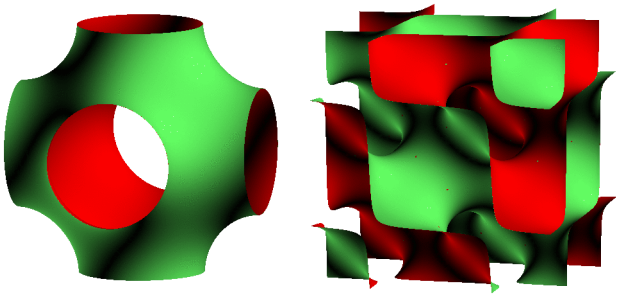

FIG. 4 (color online). Unit cells of two different minimal surfaces with a resolution of $64 \times 64 \times 64$. Left panel: Schwartz simple cubic surface. Right panel: Schwartz diamond surface.

meets all of these conditions. On the other hand, if we imposed the symmetry of the diamond lattice, we see from our subsequent numerical calculations, we would have expected to find the Schwartz D surface. Thus, provided that the composite is macroscopically isotropic at $\phi_1 = \phi_2 = 1/2$, the minimal surface that achieves the point on the upper bound is not unique. A fruitful rigorous approach to proving that these minimal surfaces are indeed optimal would be to use minimum energy principles to develop optimality conditions on the fields and ultimately on the mean curvature of the interface between the phases. Such a study will be the subject of a future paper. Note that if one breaks the symmetry of the problem by moving off the point $\phi_1 = \phi_2 = 1/2$, the optimal structure (if it exists) will still be bicontinuous but will not be a minimal surface. In future studies, it will be interesting to investigate whether such structures are bicontinuous structures with interfaces of constant mean curvature, which become minimal surfaces at the point $\phi_1 = \phi_2 = 1/2$.

Significantly, the aforementioned optimal bicontinuous composites can be made using sol-gel processing techniques [9]. Interestingly, cell membranes resembling periodic minimal surfaces have been observed in cytoplasmic organelles, such as mitochondria and chloroplasts [22], in which a variety of different transport processes occur. Our work tantalizingly suggests that it may be fruitful to explore the origins of such structures under a new light, namely, whether the optimization of competing functionalities within organelles can explain their resulting structures. Finally, note that our methodology is quite general and can be employed to discover the novel optimal microstructures that are expected to emerge when any combination of functionalities (e.g., mechanical, optical, chemical, electrical, thermal, and flow properties) compete against one another. Such analyses will lead to insights into the genesis of the optimal microstructures and will be pursued in future work.

The authors are grateful to Graeme Milton for a helpful conversation. This work was supported by the NSF MRSEC Grants No. DMR 9809483 and No. DMR 0213706.

[1] A. G. Evans, MRS Bull. **26**, 790 (2001).
[2] S. Torquato, *Random Heterogeneous Materials: Microstructure and Macroscopic Properties* (Springer-Verlag, New York, 2002).
[3] By mathematical analogy, all of our results apply to any of the pair of the following scalar effective properties: electrical conductivity, thermal conductivity, dielectric constant, magnetic permeability, and diffusion coefficient. Thus, for example, our results apply to the maximization of mass transport and flow of electricity (for instance, for intercalation cathodes in batteries).
[4] Z. Hashin and S. Shtrikman, J. Appl. Phys. **33**, 3125 (1962).
[5] M. P. Bendsoe and N. Kikuchi, Comput. Methods Appl. Mech. Eng. **71**, 197 (1988).
[6] O. Sigmund and S. Torquato, J. Mech. Phys. Solids **45**, 1037 (1997).
[7] S. Torquato and S. Hyun, J. Appl. Phys. **89**, 1725 (2001).
[8] E. L. Thomas, D. M. Anderson, C. S. Henkee, and D. Hoffman, Nature (London) **334**, 598 (1988); P. D. Olmstead and S. T. Milner, Macromolecules **31**, 4011 (1998).
[9] L. Yunfeng, Y. Yang, A. Sellinger, M. Lu, J. Huang, H. Fan, R. Haddad, G. Lopez, A. R. Burns, D. Y. Sasaki, J. Shelnutt, and C. J. Brinker, Nature (London) **410**, 913 (2001); H. Fan, C. Hartshorn, T. Buchheit, D. Tallant, R. Sullivan, S. Torquato, and C. J. Brinker (to be published).
[10] P. Ziherl and R. D. Kamien, Phys. Rev. Lett. **85**, 3528 (2000).
[11] *Micelles, Membranes, Microemulsions, and Monolayers*, W. M. Gelbart, A. Ben-Shaul, and D. Roux (Springer-Verlag, New York, 1994).
[12] D. J. Bergman, Phys. Rep. **43**, 377 (1978).
[13] G. W. Milton, J. Appl. Phys. **52**, 5294 (1981).
[14] M. Avellaneda, A. V. Cherkaev, K. A. Lurie, and G. W. Milton, J. Appl. Phys. **63**, 4989 (1988).
[15] S. Torquato, Phys. Rev. Lett. **64**, 2644 (1990); M. Avellaneda and S. Torquato, Phys. Fluids A **3**, 2529 (1991).
[16] J. G. Berryman and G. W. Milton, J. Phys. D **21**, 87 (1988); L. V. Gibiansky and S. Torquato, Phys. Rev. Lett. **71**, 2927 (1993); Proc. R. Soc. London A **452**, 253 (1996).
[17] K. Schulgasser, J. Math. Phys. (N.Y.) **17**, 378 (1976).
[18] S. Hyun, S. Torquato, and A. Donev (to be published).
[19] S. B. Vigdergauz, Mech. Solids **24**, 57 (1989); J. Appl. Mech. **3**, 300 (1994).
[20] W. T. Gozdz and R. Holyst, Phys. Rev. E **54**, 5012 (1996).
[21] See Ref. [2] for a more general definition, which is applicable to random structures at arbitrary volume fractions.
[22] National Research Council, *Biomolecular Self-Assembling Materials: Scientific and Technological Frontiers* (National Academy Press, Washington, DC, 1996).